Disentangling the Dynamical Origin of P_{11} Nucleon Resonances

N. Suzuki,[1,2] B. Juliá-Díaz,[3,2] H. Kamano,[2] T.-S. H. Lee,[2,4] A. Matsuyama,[5,2] and T. Sato[1,2]

[1]*Department of Physics, Osaka University, Toyonaka, Osaka 560-0043, Japan*
[2]*Excited Baryon Analysis Center (EBAC), Thomas Jefferson National Accelerator Facility, Newport News, Virginia 23606, USA*
[3]*Department d'Estructura i Constituents de la Matèria and Institut de Ciències del Cosmos, Universitat de Barcelona, E–08028 Barcelona, Spain*
[4]*Physics Division, Argonne National Laboratory, Argonne, Illinois 60439, USA*
[5]*Department of Physics, Shizuoka University, Shizuoka 422-8529, Japan*

(Received 23 June 2009; published 27 January 2010)

We show that two almost degenerate poles near the $\pi\Delta$ threshold and the next higher mass pole in the P_{11} partial wave of πN scattering evolve from a single bare state through its coupling with πN, ηN, and $\pi\pi N$ reaction channels. This finding provides new information on understanding the dynamical origins of the Roper $N^*(1440)$ and $N^*(1710)$ resonances listed by Particle Data Group. Our results for the resonance poles in other πN partial waves are also presented.

DOI: 10.1103/PhysRevLett.104.042302 PACS numbers: 13.75.Gx, 13.60.Le, 14.20.Gk

The excited nucleon states are unstable and couple strongly to the meson-baryon continuum states to form resonances in πN and γN reactions. Therefore, the extraction of nucleon resonances (called collectively as N^*) from data has been a well-recognized important task in advancing our understanding of strong interactions. The N^* parameters listed and periodically updated by Particle Data Group [1] (PDG) are commonly used in testing hadron structure calculations using QCD-based hadron models [2] and lattice QCD [3,4].

It is well known that resonances locate on the unphysical sheets of the complex energy plane and thus their properties can only be extracted from the empirical partial-wave amplitudes (PWA) by analytic continuation. In extracting resonances from πN data up to invariant mass $W = 2$ GeV we face a multichannel complication, namely, that a resonance may appear as a pole on more than one of the unphysical Riemann sheets, as investigated previously by Eden and Taylor [5], Kato [6], and Morgan and Pennington [7]. It is custom to name the pole which is closest to physical region as the resonance pole, and others as shadow poles. In general, the observables are mainly determined by the resonance poles. However, under certain circumstances a shadow pole could lie close to the threshold of one of the channels and could therefore affect the physical observables, as discussed in Refs. [5,7]. A theoretical understanding of the dynamical origins of these poles and their interrelations is needed to interpret the resonance parameters. In this Letter, we report progress in this direction for the N^* in the P_{11} partial wave of πN scattering. Our results for other partial waves will also be presented.

The determination of resonance poles in the P_{11} partial wave has been difficult since the discovery [8] of the Roper, $N^*(1440)$, resonance in 1964. It was first found by Arndt, Ford, and Roper [9] that this partial wave has two almost degenerate poles near the $\pi\Delta$ threshold. This was confirmed and investigated in more detail by Cutkosky and Wang [10]. This two pole structure has also been obtained in the recent analysis by the GWU/VPI [11] and Jülich [12] groups. In this Letter, we demonstrate that these two poles near the $\pi\Delta$ threshold ($\sim$1360 MeV) and a pole at about 1800 MeV correspond to a single bare state within a dynamical coupled-channels model (JLMS) developed in Ref. [13]. Thus they have the resonance pole-shadow pole relation as discussed in Refs. [5–7]. Our result suggests that the $N^*(1440)$ and $N^*(1710)$ listed by PDG originate from the same excited nucleon state modeled as a bare particle within the JLMS model.

The JLMS model is defined within a Hamiltonian formulation [14] of multichannel reactions. It describes meson-baryon (MB) reactions involving the following channels: πN, ηN, and $\pi\pi N$ which has $\pi\Delta$, ρN, and σN resonant components. The excitation of the internal structure of a baryon (B) by a meson (M) to a bare N^* state is modeled by a vertex interaction $\Gamma_{MB\leftrightarrow N^*}$. The Hamiltonian also has energy independent interactions $v_{MB,M'B'}$ which describe the meson-exchange mechanisms deduced from phenomenological Lagrangians. Nucleon resonances can be due to the $MB \to N^* \to M'B'$ transitions induced by the vertex interaction $\Gamma_{MB\leftrightarrow N^*}$ in this formulation. But they can also be due to the attractive forces of $v_{MB,M'B'}$ and channel coupling effects. For investigating the N^* structure, the second type of resonances, called molecular-type resonances in the literature, must also be identified in the analysis. For the same consideration, the parametrization of $v_{MB,M'B'}$, in particular, their phenomenological form factors, must be carefully constrained by the data. This had been achieved by performing rather complex χ^2 fits to the πN scattering data, as detailed in Ref. [13]. Briefly, the JLMS model is able to describe the data of πN elastic scattering up to invariant mass $W = 2$ GeV. The resulting πN scattering amplitudes and total cross sections are in good agreement with those from

SAID [11]. Furthermore, the predicted 2π production cross sections [15] are in good agreement with the available data.

Within the JLMS model, it is convenient to cast the partial-wave amplitude of the $M(\vec{k}) + B(-\vec{k}) \to M'(\vec{k}') + B'(-\vec{k}')$ reaction into the following form (suppressing the angular momentum and isospin indices):

$$T_{MB,M'B'}(k, k', E) = t_{MB,M'B'}(k, k', E) + t^{N^*}_{MB,M'B'}(k, k', E), \tag{1}$$

where the first term (called meson-exchange amplitude from now on) is defined by

$$t_{MB,M'B'}(k, k', E) = v_{MB,M'B'}(k, k') + \sum_{M''B''} \int_{C_{M''B''}} q^2 dq v_{MB,M''B''}(k, q) G_{M''B''}(q, E) t_{M''B'',M'B'}(q, k'E), \tag{2}$$

where C_{MB} is the integration contour in the complex-q plane used for channel MB. The term associated with the bare N^* states in Eq. (1) is

$$t^{N^*}_{MB,M'B'}(k, k', E) = \sum_{N^*_i, N^*_j} \bar{\Gamma}_{MB \to N^*_i}(k, E) \times [D(E)]_{i,j} \bar{\Gamma}_{N^*_j \to M'B'}(k', E), \tag{3}$$

where $\bar{\Gamma}_{N^*_j \to M'B'}(k, E)$ is the dressed vertex function which is calculated [13] from the bare vertex $\Gamma_{N^*_j \to M'B'}(k)$ and convolutions over the meson-exchange amplitudes $t_{MB,M'B'}(k, k', E)$. The inverse of the propagator of dressed N^* states in Eq. (3) is $[D^{-1}(E)]_{i,j} = (E - M^0_{N^*})\delta_{i,j} - [M(E)]_{i,j}$, where $M^0_{N^*_i}$ is the bare mass of the ith N^* state, and the N^* self-energy is defined by

$$[M(E)]_{i,j} = \sum_{MB} \int_{C_{MB}} q^2 dq \bar{\Gamma}_{N^*_j \to MB}(q, E) G_{MB}(q, E) \times \Gamma_{MB \to N^*_i}(q, E). \tag{4}$$

Defining $E_\alpha(k) = [m^2_\alpha + k^2]^{1/2}$ with m_α being the mass of particle α, the meson-baryon propagators in the above equations are $G_{MB}(k, E) = 1/[E - E_M(k) - E_B(k) + i\epsilon]$ for the stable πN and ηN channels, and $G_{MB}(k, E) = 1/[E - E_M(k) - E_B(k) - \Sigma_{MB}(k, E)]$ for the unstable $\pi\Delta$, ρN, and σN channels. The self-energy $\Sigma_{MB}(k, E)$ is calculated from a vertex function defining the decay of the considered unstable particle in the presence of a spectator π or N with momentum k. For example, we have for the $\pi\Delta$ state,

$$\Sigma_{\pi\Delta}(k, E) = \frac{m_\Delta}{E_\Delta(k)} \int_{C_3} q^2 dq \frac{M_{\pi N}(q)}{[M^2_{\pi N}(q) + k^2]^{1/2}} \times \frac{|f_{\Delta \to \pi N}(q)|^2}{E - E_\pi(k) - [M^2_{\pi N}(q) + k^2]^{1/2} + i\epsilon}, \tag{5}$$

where $M_{\pi N}(q) = E_\pi(q) + E_N(q)$ and $f_{\Delta \to \pi N}(q)$ defines the decay of the $\Delta \to \pi N$ in the rest frame of Δ, C_3 is the corresponding integration contour in the complex-q plane. The self-energies for ρN and σN channels are similar.

To search for resonance poles, we need to choose the contours C_{MB} and C_3 appropriately to solve Eqs. (2)–(5) for E on the various possible unphysical sheets of the Riemann surface. This requires careful examinations of the locations of the on-shell momentum of each propagator $G_{MB}(k, E)$ and the $\pi\pi N$ cut in the self-energies, such as $\Sigma_{\pi\Delta}(k, E)$ of Eq. (5), of the unstable particle channels. Furthermore, we need to account for the singularities of $v_{MB,M'B'}(k, k')$ of Eq. (2) on the chosen contours. Our method was tested [16] within several exactly solvable models. Like all previous works [11,17], we only look for poles which are close to the physical region and have effects on πN scattering observables. All of these poles are on the unphysical sheet of the πN channel, but could be on either unphysical (u) or physical (p) sheets of other channels considered in this analysis. We will indicate the sheets where the identified poles are located by ($s_{\pi N}$, $s_{\eta N}$, $s_{\pi\pi N}$, $s_{\pi\Delta}$, $s_{\rho N}$, $s_{\sigma N}$), where s_{MB} and $s_{\pi\pi N}$ can be u or p or—denoting no coupling to this channel.

Equation (1) indicates that if no pole is found in the first term $t_{\pi N,\pi N}(k, k', E)$, then the poles of the total amplitude can be found from the second term $t^{N^*}_{\pi N,\pi N}(k, k', E)$. But if $t_{\pi N,\pi N}(k, k', E)$ has a pole, we need to check whether it will be canceled by the second term, as demonstrated in Ref. [12]. Thus our procedure is to first use the standard method to determine whether $t_{\pi N,\pi N}(k, k', E)$ has poles by examining the determinant of $[1 - vG]^{-1}$ of Eq. (2). It turns out that we do not find any pole from these meson-exchange amplitudes. Thus there is no molecular-type nucleon resonance within JLMS model.

We thus can search for poles of the total amplitudes from finding the zeros of the determinant of $D^{-1}(E)$. Here we use the well-established Newton iteration method. We have performed searches in the $(m_\pi + m_N) \le \mathrm{Re}(E) \le 2000$ MeV and $-\mathrm{Im}(E) \le 250$ MeV region within which PDG's 3- and 4-star resonances are listed. Poles with very large widths are more difficult to locate precisely with our numerical methods and hence will not be discussed here.

We now focus on our results in P_{11} partial wave. We find two poles near the PDG value $(\mathrm{Re}M_R, -\mathrm{Im}M_R) = (1350\text{–}1380, 80\text{–}110)$ of the Roper, $N^*(1440)$, resonance. This finding is consistent with the results from the analysis by Cutkosky and Wang [10] (CMB), GWU/VPI [11] and Jülich [12] groups, as seen in Table I. In our analysis, we find that they are on different sheets: (1357, 76) and (1364, 105) are on the unphysical and physical sheet of the $\pi\Delta$ channel, respectively.

We also find one higher mass pole at (1820, 248) in P_{11} partial wave, which is close to the $N^*(1710)$ state listed by PDG. Within the JLMS model, we find that this pole and the two poles listed in Table II are related to one of the two bare states needed to obtain a good fit to the P_{11} amplitude up to $W = 2$ GeV, see [13]. To see how these poles evolve

TABLE I. P_{11} resonance pole positions M_R [listed as (ReM_R, $-$ImM_R)] extracted from four different approaches are compared.

Analysis	P_{11} poles (MeV)	
JLMS [13]	(1357, 76)	(1364, 105)
CMB [10]	(1370, 114)	(1360, 120)
GWU/VPI [11]	(1359, 82)	(1388, 83)
Jülich [12]	(1387, 74)	(1387, 71)

dynamically through their coupling with reaction channels, we trace the zeros of $\det[\hat{D}^{-1}(E)] = \det[E - M^0_{N^*} - \sum_{MB} y_{MB} M_{MB}(E)]$ in the region $0 \leq y_{MB} \leq 1$, where $M_{MB}(E)$ is the contribution of channel MB to the self-energy defined by Eq. (4). Each y_{MB} is varied independently to find continuous evolution paths through the various Riemann sheets on which our analytic continuation method is valid.

We find that the three poles listed in Table I are associated to the bare state at 1736 MeV as shown in Fig. 1. The solid blue curve shows the evolution of this bare state to the position at $C(1820, 248)$ on the unphysical sheet of the $\pi\Delta$ and ηN channels. The poles $A(1357, 76)$ and $B(1364, 105)$ evolve from the same bare state on the physical sheet of the ηN channel. The dashed red curve indicates how the bare state evolves through varying all coupling strengths except keeping $y_{\pi\Delta} = 0$, to about Re$(M_R) \sim 1400$ MeV. By further varying $y_{\pi\Delta}$ to 1 of the full JLMS model, it then splits into two trajectories; one moves to pole $A(1357, 76)$ on the unphysical sheet and the other to $B(1364, 105)$ on the physical sheet of $\pi\Delta$ channel. Figure 1 clearly shows how the coupled-channels effects induces multipoles from a single bare state. The evolution of the second bare state at 2037 MeV [13] into a resonance at $W > 2$ GeV can be similarly investigated, but will not be discussed here.

To explore this interesting result further and to examine the stability of the determined three P_{11} poles, we have performed several refits of the P_{11} amplitudes within the JLMS model. We are able to get new fits by varying solely the parameters associated with the bare N^* state at 1763 MeV while keeping its bare mass value varied within the range 1763 ± 100 MeV. The quality of these fits is comparable to that of the original JLMS model. The above described features remain unchanged: we find in all refitted results two poles close to the $\pi\Delta$ threshold, within 1 MeV of the positions reported in Table II. The third higher mass pole is also found but its position varies up to 30 MeV from the value given in Table II. The trajectories similar to that shown in Fig. 1 are also obtained. This is the extent to which the stability of the resonance pole-shadow pole relation among the three P_{11} poles we can establish here. A more detailed analysis of the model dependence of our results would involve extensive refits by varying the parameters associated with both the meson-exchange interaction $v_{MB,M'B'}$ and bare N^* states in all partial waves and can not be addressed here.

TABLE II. The resonance pole positions M_R [listed as (ReM_R, $-$ImM_R)] extracted from the JLMS model in the different unphysical sheets are compared with the values of 3- and 4-star nucleon resonances listed in the PDG [1]. The notation indicating their locations on the Riemann surface are explained in the text. "$\cdots$" for $P_{33}(1600)$, P_{13}, and P_{31} indicates that no resonance pole has been found in the considered complex energy region. All masses are in MeV.

	$M^0_{N^*}$	M_R	Location	PDG
S_{11}	1800	(1540, 191)	($uuuupp$)	(1490–1530, 45–125)
	1880	(1642, 41)	($uuuupp$)	(1640–1670, 75–90)
P_{11}	1763	(1357, 76)	($upuupp$)	(1350–1380, 80–110)
	1763	(1364, 105)	($upuppp$)	
	1763	(1820, 248)	($uuuuup$)	(1670–1770, 40–190)
P_{13}	1711	$\cdots$		(1660–1690, 57–138)
D_{13}	1899	(1521, 58)	($uuuupp$)	(1505–1515, 52–60)
D_{15}	1898	(1654, 77)	($uuuupp$)	(1655–1665, 62–75)
F_{15}	2187	(1674, 53)	($uuuupp$)	(1665–1680, 55–68)
S_{31}	1850	(1563, 95)	(u-uup-)	(1590–1610, 57–60)
P_{31}	1900	$\cdots$		(1830–1880, 100–250)
P_{33}	1391	(1211, 50)	(u-ppp-)	(1209–1211, 49–51)
	1600	$\cdots$		(1500–1700, 200–400)
D_{33}	1976	(1604, 106)	(u-uup-)	(1620–1680, 80–120)
F_{35}	2162	(1738, 110)	(u-uuu-)	(1825–1835, 132–150)
	2162	(1928, 165)	(u-uuu-)	
F_{37}	2138	(1858, 100)	(u-uuu-)	(1870–1890, 110–130)

To further compare our P_{11} poles with the $N^*(1440)$ and $N^*(1710)$ listed by PDG, we have applied the method explained in Ref. [16] to extract the residues $F = \mathrm{Re}^{i\phi}$ which is related to S matrix by $S(E) \rightarrow 1 + 2iF/(E - M_R)$ as $E \rightarrow M_R$. We obtain $(R[\mathrm{MeV}], \phi[\mathrm{degrees}]) = (36, -111)$, $(64, -99)$, $(20, -168)$ for the P_{11} poles at $(\mathrm{Re}M_R, -\mathrm{Im}M_R) = (1357, 76)$, (1364, 105), and (1820, 248), respectively. The branching ratio of the N^* decay into πN channel can then be estimated by evaluating $\eta_e \sim R/(-\mathrm{Im}(M_R))$. Our results for the P_{11} poles at (1357, 76) and (1364, 105) are 49% and 61%, respectively. These values are close to 60%–70% of the $N^*(1440)$ listed by PDG. Our result for the pole at (1820, 248) is 8% which is also close to 10%–20% of $N^*(1710)$. We thus have firmer evidence showing that these two N^* states listed by PDG do evolve from the same bare state through its coupling with πN, ηN, and $\pi\pi N$ reaction channels.

Let us now turn to other partial waves. In Table II, the extracted resonance poles positions (M_R) are compared with the bare N^* masses ($M^0_{N^*}$) of the JLMS model and the 3- and 4-star values listed by PDG [1]. With the exception of the $P_{33}(1600)$, P_{13}, and P_{31} cases, all pole positions listed by the PDG are consistent with our results. One possible reason for not finding these poles is that their imaginary part may be beyond the $-\mathrm{Im}(M_R) \leq 250$ MeV region where our analytic continuation method is accurate and is covered in our searches. Another possibility is that these resonances, if indeed they exist, are perhaps due to the mechanisms which are beyond the JLMS model, but

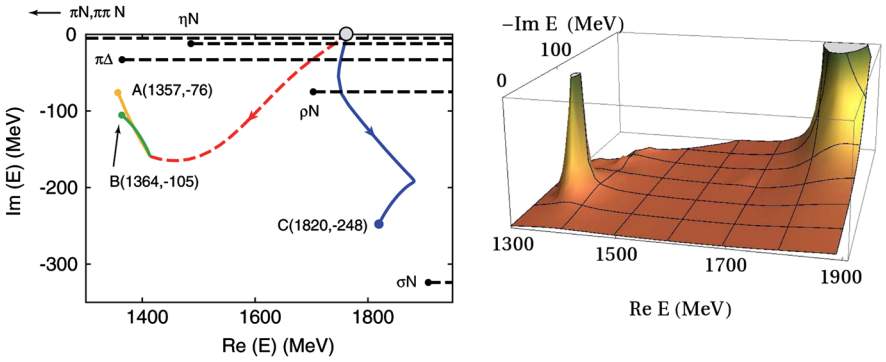

FIG. 1 (color online). (left) Trajectories of the evolution of P_{11} resonance poles $A(1357, 76)$, $B(1364, 105)$, and $C(1820, 248)$ from a bare N^* with 1763 MeV, as the couplings of the bare N^* with the meson-baryon reaction channels are varied from zero to the full strengths of the JLMS model. See text for detailed explanations. Brunch cuts for all channels are denoted as dashed lines. The branch points, $E_{\text{b.p.}}$, for unstable channels are determined by $E_{\text{b.p.}} - E_M(k) - E_B(k) - \Sigma_{MB}(k, E_{\text{b.p.}}) = 0$ of the their propagators (described in the text) evaluated at the spectator momentum $k = 0$. With the parameters [14] used in JLMS model, we find that $E_{\text{b.p.}}(\text{MeV}) = (1365.40, -32.46), (1704.08, -74.98), (1907.57, -323.62)$ for $\pi\Delta$, ρN, and σN, respectively. (right) Three-dimensional depiction of the behavior of $|\det[D(E)]|^2$ of the P_{11} N^* propagator (in arbitrary units) as a function of complex E.

are particularly sensitive to these partial waves. On the other hand, the possibility that these resonances do not exist cannot be excluded since the πN data are not complete and all partial-wave analyses involve unavoidable theoretical assumptions. For the F_{35} partial wave, we have also analyzed the evolution trajectories and found that the two poles listed in Table II correspond to the same bare state at 2162 MeV.

In summary, we have applied an analytic continuation method [16] to extract nucleon resonances from a dynamical coupled-channels model within which the bare N^* states were determined from fitting the πN scattering data up to $W = 2$ GeV [13]. Compared with all previous analysis, the new aspect of this work is to study the evolution of resonance pole parameters as a function of the coupling to continuum meson-baryon channels. Our most important finding is that the two lowest P_{11} nucleon resonances, the Roper $N^*(1440)$ and $N^*(1710)$, originate from a single bare state. Our finding has an important implication in understanding how nucleon resonances arise in QCD. It implies that in some limits in which the coupling to the continuum is not fully implemented, for example, large N_c QCD or quenched lattice QCD, there could be fewer nucleon resonances. Another possible implication is that the bare N^* states, not the resonance poles, determined within our model could correspond to hadron structure calculations which exclude the coupling with meson-baryon continuum. Further investigations of these possibilities as well as related theoretical questions are needed to open a new direction towards understanding nucleon resonances and their connection to QCD. Finally, we mention that our results have confirmed most of the 3- and 4-star nucleon resonance poles listed by PDG but found no evidence of two four-star resonances, $P_{13}(1720)$, $P_{31}(1910)$, and one three-star one, $P_{33}(1600)$.

This work is supported by the JSPS, Kakenhi, (C) 20540270, by the U.S. D.O.E. Nuclear Physics Division Contract No. DE-AC02-06CH11357, and Contract No. DE-AC05-060R23177 under which Jefferson Science Associates operates Jefferson Lab, and by a CPAN CSD 2007-0042 contract, by Grants No. FIS2008-1661 (Spain).

[1] C. Amsler *et al.*, Phys. Lett. B **667**, 1 (2008).
[2] N. Isgur and G. Karl, Phys. Rev. D **19**, 2653 (1979); S. Capstick and W. Roberts, Prog. Part. Nucl. Phys. **45**, S241 (2000); L. Y. Glozman and D. O. Riska, Phys. Rep. **268**, 263 (1996); C. D. Roberts, Prog. Part. Nucl. Phys. **61**, 50 (2008).
[3] S. Dürr *et al.*, Science **322**, 1224 (2008).
[4] K. Sasaki and S. Sasaki, Phys. Rev. D **72**, 034502 (2005).
[5] R. J. Eden and J. R. Taylor, Phys. Rev. Lett. **11**, 516 (1963).
[6] M. Kato, Ann. Phys. (N.Y.) **31**, 130 (1965).
[7] D. Morgan and M. R. Pennington, Phys. Rev. Lett. **59**, 2818 (1987).
[8] L. D. Roper, Phys. Rev. Lett. **12**, 340 (1964).
[9] R. A. Arndt, J. M. Ford, and L. D. Roper, Phys. Rev. D **32**, 1085 (1985).
[10] R. E. Cutkosky and S. Wang, Phys. Rev. D **42**, 235 (1990).
[11] R. A. Arndt, W. J. Briscoe, I. I. Strakovsky, and R. L. Workman, Phys. Rev. C **74**, 045205 (2006).
[12] M. Doring *et al.*, Nucl. Phys. **A829**, 170 (2009).
[13] B. Julia-Diaz, T.-S. H. Lee, A. Matsuyama, and T. Sato, Phys. Rev. C **76**, 065201 (2007).
[14] A. Matsuyama, T. Sato, and T.-S. H. Lee, Phys. Rep. **439**, 193 (2007).
[15] H. Kamano, B. Julia-Diaz, T.-S. H. Lee, A. Matsuyama, and T. Sato, Phys. Rev. C **79**, 025206 (2009).
[16] N. Suzuki, T. Sato, and T.-S. H. Lee, Phys. Rev. C **79**, 025205 (2009); arXiv 0910.1742.
[17] T. P. Vrana, S. A. Dytman, and T.-S. H. Lee, Phys. Rep. **328**, 181 (2000).